

## 7 Tesla in vivo of the Human Eye: A SNR and CNR Optimization Study

P. A. Wassenaar<sup>1</sup>, K. Richdale<sup>2</sup>, K. T. Bluestein<sup>1</sup>, J. Christoforidis<sup>3</sup>, T. Lanz<sup>4</sup>, M. V. Knopp<sup>1</sup>, and P. Schmalbrock<sup>1</sup>

<sup>1</sup>Radiology, The Ohio State University, Columbus, OH, United States, <sup>2</sup>Optometry, The Ohio State University, Columbus, OH, United States, <sup>3</sup>Ophthalmology, The Ohio State University, Columbus, OH, United States, <sup>4</sup>Rapid MR International, LLC, Columbus, OH, United States

### Introduction

High quality ocular imaging is critical for understanding and diagnosing diseases of the eye. Optimal eye imaging techniques have to be capable of very high spatial resolution for depiction of small anatomical structures, and to allow for fast scan times minimizing eye motion artifacts [Bert, Patz]. The increased SNR makes 7T MRI uniquely suited for this task. The objective of our study was to optimize 7T ocular MRI with a dedicated eye coil for two sequences, 3D spoiled gradient echo imaging (3D-SPGR) and 3D inversion prepared turbo-field echoes (IR-TFE), which tend to outperform other sequences at ultrahigh field MRI due to lower SAR requirements and decreased sensitivity to RF inhomogeneity.

### Methods

Ten healthy subjects (2f/8m, 26-54y) were imaged under IRB approval at 7T (Philips, Achieva) using a volume head coil (Nova Medical) for transmission, and dedicated single loop 4cm receive coil (Rapid International, Columbus, OH). Different eye positions (open/close) and focusing were explored. To aid sequence optimization, T1 were measured with moderate resolution using 3D-SPGR (TR/TE=20/2.9ms; flip angles 5-40°; 0.25x0.25x1.0mm<sup>3</sup>), and with 3D-IR-TFE (inversion pulse interval TS=5000ms; TI=450-3200ms, 0.4x0.4x1.6 mm<sup>3</sup>). T1 values were computed for manually traced ROI using Wang's linear fitting method [Wang] with flip angles corrected from measured B1-maps and exponential fitting for IR-TFE. Resulting T1 and scaling factors (const-PD-exp(-TE/T2\*)) were used to estimate optimal sequence parameter producing shortest scan time. High resolution images were subsequently acquired with optimized parameters for 3D-SPGR and 3D-IR-TFE.

### Results

Figure 1 demonstrates contrast behavior for the SPGR sequence. For optimal depiction of the lens and ciliary body, best results were achieved with high signal in these structures while suppressing signal from the surrounding aqueous and vitreous humor. Eye imaging at 7T is extremely sensitive to motion and susceptibility. Severe artifacts from air/tissue interfaces at the eyelids can obscure the anterior chamber and lens. To compensate for susceptibility artifacts, the imaged eye was held closed with adhesive tape and the subject was asked to fixate with the contralateral eye such that the imaged eye pointed predominantly behind the closed lid. Susceptibility artifacts were further reduced by using thin-section 3D imaging and minimum TE. Motion artifacts were reduced by phase encoding in the AP direction [Patz] and the use of very short scan times [Patz, Berkowitz]. Signal simulations indicated best results for 3D-SPGR with TR/flip=10/20° and 35 sec scan time for 0.15x0.25x1.0 voxel size (420x260x3 matrix) yielding SNR 12.8, and for 3D-IR-TFE TS/TI=2000/1000ms and 34 sec scan time yielding SNR 8.5. To increase SNR, these short scans were repeated 12-16 times with a 2 second interval between repeats to allow for blinking and relaxation of accommodation. Image sets were registered in 3D using FSL and added to achieve final SNR of 41 and 32 for 3D-SPGR (Fig 2 Left) and 3D-IRTFE (Fig 2 Right), respectively.

### Discussion

Optimization of pulse sequences and avoidance of susceptibility and motion artifacts led to high quality images of with a spatial resolution and SNR exceeding prior standard field (1.5T) work. Ocular imaging at 7T with a dedicated eye coil improves delineation of the fine ocular structures. This ability is an essential improvement to assess retinal changes associated with diabetes and macular degeneration, or to study the mechanism of refractive error and presbyopia, all projects that will be enabled with this improved imaging approach.

### References

[1] Bert RJ, et al, Acad Radiol 12:368-378 (2006); [2] Patz S, et al, JMRI 26:510-518 (2007); [3] Wang HZ, et al, MRM 5: 399-416 (1987); [4] Berkowitz BA, et al, NMR Biomed (2008).

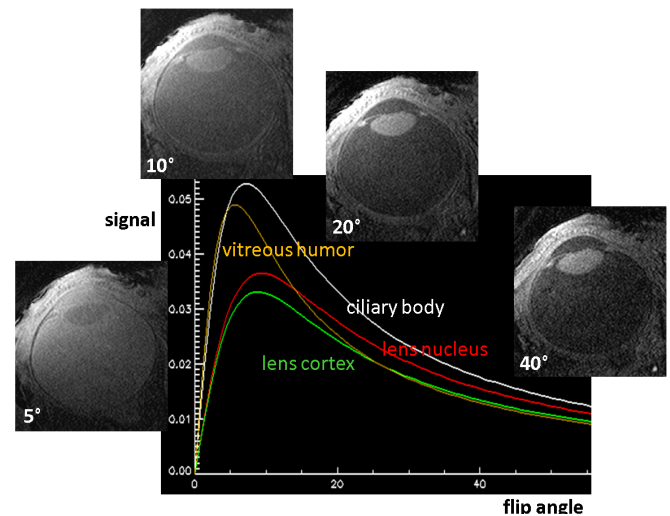


Figure 1: Numerical simulation of signal intensities of ocular structures for a SPGR sequence with variable flip angles. Illustrated are acquired images with indicated flip angles.

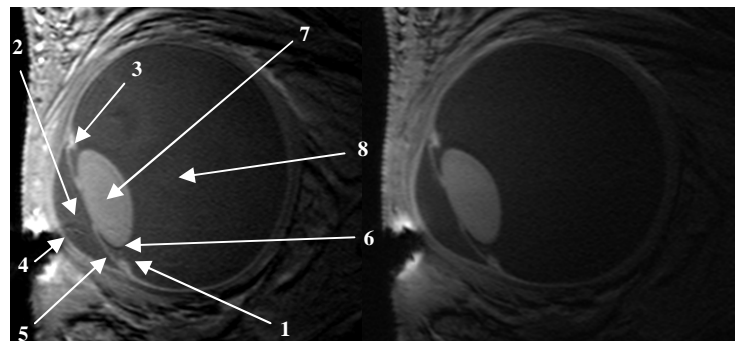


Figure 2 Left: SPGR with locations of ROIs: (1) posterior chamber, (2) anterior chamber, (3) ciliary body, (4) cornea, (5) iris, (6) lens cortex, (7) lens nucleus, (8) vitreous humor. Note the visible susceptibility artifact near the air-eyelid interface. Figure 2 Right: IR-TFE sequence.